CHAPTER 6

In silico Investigation on the Conformational Dynamics of N-Terminal Lid of MDM2 in the presence and absence of p53 C-Terminal Domain

In silico Investigation on the Conformational Dynamics of N-Terminal Lid of MDM2 in the presence and absence of p53 C-Terminal Domain

6.1. Abstract:

The MDM2 protein is the main antagonist of the p53 molecule, which is a tumor suppressor protein. The primary site of interaction between p53 and MDM2 has been well studied. But there exists a secondary site of interaction between the CTD of p53 N-Terminal Lid present in the NTD of MDM2, which aids to the stability of the complex. Here, we have studied the conformational dynamics and stability of the NTD of MDM2 with the lid, and the p53(CTD)-MDM2(NTD) complex using molecular dynamics (MD) simulation. It was found that the NTD of MDM2 with the lid remains in closed conformation throughout the simulation, while the N-Terminal lid in the p53(CTD)-MDM2(NTD) complex gets displaced throughout the simulation and the initial closed conformation of the p53(CTD)-MDM2(NTD) complex gets shifted to an open conformation at the end of the simulation. We then docked the p53 TAD1 with the lowest energy structure of the p53(CTD)-MDM2(NTD) complex, and it was found that the p53 TAD1 fits exactly into the N-Terminal binding cavity of MDM2. The findings from our study may be beneficial in designing novel potential inhibitors for disrupting the p53-MDM2 interactions.

6.2. Introduction:

p53 is a major tumor suppressor protein. It is involved in the regulation of cell proliferation, cell death, and cell differentiation. The p53 protein is activated by an overabundance of cellular stresses such as oncogene activation, hypoxia, DNA damage, replicative stress [587]. The activation mechanism includes posttranslational modifications that inhibit MDM2 from degrading p53, and enhance the p53 DNA binding affinity. When activated, p53 tetramers attach to responsive elements in genomic DNA, causing a cascade of target genes to be transcribed, orchestrating stress tolerance, cell cycle arrest, repair of the DNA, tumor suppression, and apoptosis [588]. Mutations are found in p53 in about 50% of human tumors. The transcriptional activity of the mutated p53 is lost and new functions driving tumor progression are gained [589].

The p53 protein is made up of multiple structural as well as functional domains. The NTD, comprising of 90 residues, consists of two TADs (TAD1: 1–40, TAD2: 40–60) followed by a proline-rich region (PRR: 60–90) [589]. TAD1 consists of the primary binding site for MDM2 protein. TAD2 is required in the transcription activation as well as protein interactions. TAD1 and TAD2 mutations are necessary to terminate the tumor suppressing function [590]. Many phosphorylation sites are present in the TAD1 and TAD2 of p53 responsible for regulating p53 degradation as well as activity throughout stress response. PRR with mutations or deletions compromise growth suppression, tumor suppression, transactivation, p53 degradation, and apoptosis [591-593]. The core DBD (residues: 94–312) is necessary for sequence-specific DNA binding. It is also the target of majority of the point mutations in cancer. The C terminus (CT: 312–393) comprises of an oligomerization domain (OD: 323–355) followed by a lysine-rich C-terminal tail (CTD: 364–393) that comprises of sites for phosphorylation, methylation, and acetylation.

MDM2 is a primary negative regulator of p53, exhibits both p53-independent and p53- dependent functions. The functions of MDM2 are revealed via its domain architecture. The N-terminal region is required for interacting with p53 and preventing it from becoming transcriptionally active. A nuclear localization signal (NLS) at position 178 followed by a nuclear export signal (NES) at location 192 make up the linker region that follows the NTD. The central AD plays an important supporting function in p53 degradation [594-596]. The zinc-finger domain comes next, and it is supposed to help with interactions with many proteins, such as nucleolar and ribosomal proteins [597], and tumor suppressor p14ARF. A RING (Really Interesting New Gene) domain (amino acids 436–482) comprises of a nucleolar localization signal (NoLS; residues 466–473). The RING domain as well as residues present at the C terminus tail (amino acids 485–491) make up the MDM2 C terminus [598, 599]. The C terminus tail plays an important role in inter RING domains interactions. The RING domain of MDM2 is important for the protein's E3 ligase activity, which is required for MDM2 to restrict the p53 molecules during early embryogenesis.

A mutual regulation exists between p53 and MDM2 molecules, which is maintained by a feedback loop [600]. When any stimuli or any DNA damage activates the p53 molecules, the transcription rate is increased for the MDM2 mRNAs and proteins resulting in the binding of MDM2 to p53, which directly inhibits the functioning of p53

molecules by three primary mechanisms. First, MDM2 (an E3 ligase) ubiquitinates the p53 molecules, which results in the proteasomal degradation of p53 molecules. Second, the NTD of MDM2 binds to the TAD1 of p53, which is the primary site of interaction between p53 and MDM2, hindering p53 from binding to its target DNA, which results in a lack of transcription. Third, the p53 molecules are exported fast from the nucleus of the cell by the MDM2 molecules, making the p53 molecules inaccessible to the nuclear target DNA mandatory for transcription. Remarkably, the mutations in the Tumor Protein 53 (*TP53*) and gene amplification of MDM2 are found to be mutually exclusive in human cancers.

Apart from the primary site of interaction between the p53 and MDM2 molecules, there exists a secondary site of interaction these molecules. This secondary interaction occurs between the central AD of MDM2 and the core DBD of p53. And this interaction is essential for targeting p53 for proper ubiquitination [601-606]. Another secondary site of interaction between p53 and MDM2 exists between the N-Terminal Lid of MDM2 and the CTD of p53 [297]. Poyurovsky *et al*., 2010 also predicted that binding of the p53 CTD to the N-Terminal Lid region present in the N-Terminus of MDM2, which predominantly exists in closed conformation in apo state, would disrupt the intramolecular links made by the lid region and then enable the transformation of MDM2 to an open conformation, thus allowing the binding of the p53 TAD1 domain.

In the present study, the conformational dynamics and stability of the two systems: MDM2 NTD (Apo) and the p53 CTD - MDM2 N-terminal Lid (p53-MDM2) complex have been studied using molecular dynamics (MD) simulation.

6.3. Materials & Methods:

6.3.1. Molecular docking and the preparation of initial structures:

The 3D structure of p53 CTD has been modelled using the FASTA sequence of Human p53 protein retrieved from UniProt database (UniProt ID: P04637), and then submitting the FASTA sequence (residues: 364-393) to the I-TASSER server. Five models were then obtained. The best structure was then viewed using the UCSF Chimera software v.1.13.1.

The 3D structure of the MDM2 NTD has been downloaded from RCSB PDB (PDB ID: 1Z1M). The modelled 3D structure of p53 CTD was then docked with the 3D

structure of MDM2 NTD using ClusPro 2.0 online server. The complex structure with the best model score was chosen as the initial structure for the further analyses.

6.3.2. Setup for MD simulations:

The two systems: (1) MDM2 (Apo), and (2) MDM2(NTD)-p53(CTD) complex were prepared for the molecular dynamics (MD) simulation using the AMBER ff99SB force field using the Leap module of the AMBER 14 software package. The rest of the steps were performed as mention in section **4.3.2**.

6.3.3. Analysis of the MD Trajectories:

The analysis of the MD trajectories have been performed using the modules mentioned in section **4.3.3**.

6.3.4. BFE and PRED analysis:

In this work, the BFE and PRED of the p53(CTD)-MDM2(NTD) complex interface residues were determined using the procedure mentioned in section **4.3.6.**

6.4. Results & Discussions:

6.4.1. Analysis of the conformational dynamics of MDM2 in apo and in p53-MDM2 complex states:

MD simulations provide in-depth knowledge about the dynamic characteristics of a specific system under study, and assist us in understanding changes in their flexibility and stability with respect to time.

The snapshots of the MDM2 NTD structures and the snapshots of the p53-MDM2 complex structures were created from the MD trajectories of the 50 ns simulation, at intervals of 5 ns using UCSF Chimera (as shown in **Figure 6.1** and **6.2** respectively).

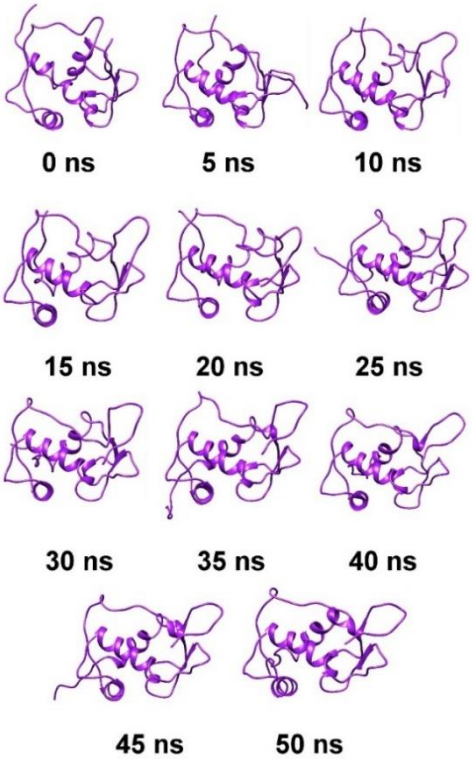

Figure 6.1. *Snapshots of MDM2 N-Terminal Domain (Apo) during 50 ns MD simulation.*

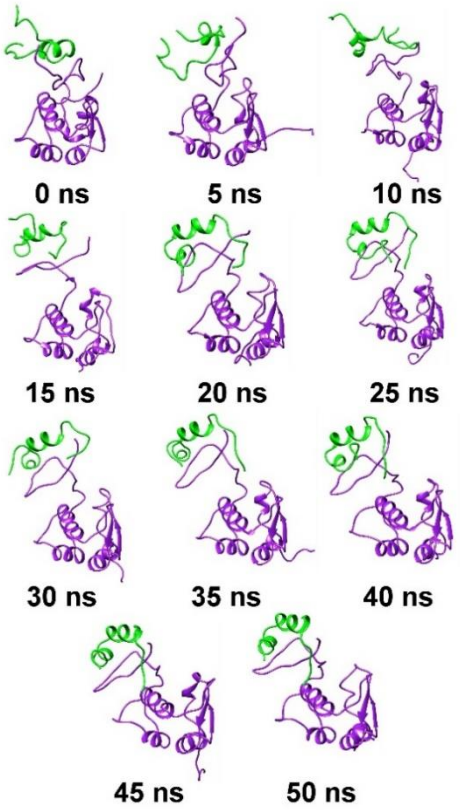

Figure 6.2. *Snapshots of MDM2 N-Terminal Domain (Apo) during 50 ns MD simulation.*

The lowest energy structure of the p53(CTD)-MDM2(NTD) complex was then docked with the p53 TAD1 using ClusPro 2.0 online server. The p53 TAD1 fits exactly in the N-Terminal binding cavity of MDM2 (**Figure 6.3a**). On the other hand, the lowest energy structure of the p53(CTD)-MDM2(NTD) complex was then superimposed with structure of p53-MDM2 complex downloaded from RCSB PDB (PDB ID: 1YCR). The superimposed p53 TAD1 occupies the N-Terminal binding cavity of MDM2 in the same manner as the docked p53 TAD1 (**Figure 6.3b**).

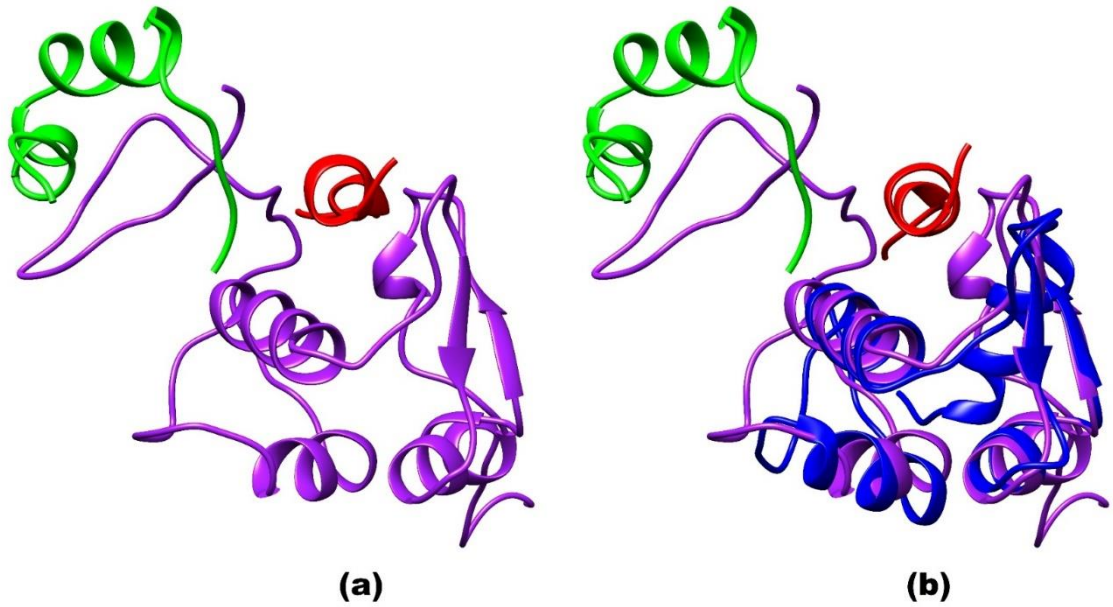

Figure 6.3. *The Lowest Energy structure of p53(CTD)-MDM2(NTD) complex (a) docked with p53 TAD1, and (b) superimposed with the structure of MDM2 Bound to the Transactivation Domain of p53 (PDB ID: 1YCR).*

MD simulation was carried out for both MDM2 (Apo) and p53-MDM2 complex for 50 ns to study the salient structural features of the two systems: RMSD, RMSF, Rg, SASA, and Hydrogen Bond analyses.

6.4.2. RMSD Analysis:

In a usual MD simulation, the stability of the system is usually determined by the RMSD of the protein/biological molecule with respect to time. For the two systems studied: MDM2 (Apo) and p53-MDM2 complex, the RMSD values with respect to time have been shown in **Figure 6.4a** and **6.4b** respectively. For the two systems, the RMSD analysis for

the N-Terminal lid of MDM2 has been shown in **Figure 6.4c** and **6.4d**. **Figure 6.4b** represents a comparative RMSD plot for the p53 (CTD), MDM2 (NTD), and p53-MDM2 complex. The MDM2 (Apo) was found to have converged at 5 ns with the average CoM distance of 6 Å. The p53 (CTD), MDM2 (NTD), and p53-MDM2 complex were found to have converged at 2.5 ns, 17.5 ns, and 17.5 ns with the average CoM distance of 3 Å, 9 Å, and 11 Å, respectively. The N-Terminal lid of MDM2 (Apo) was found to have converged at 2.5 ns with the average CoM distance of 6 Å, and the N-Terminal lid of MDM2 (p53-MDM2) was found to have converged at 30 ns with the average CoM distance of 12.5 Å.

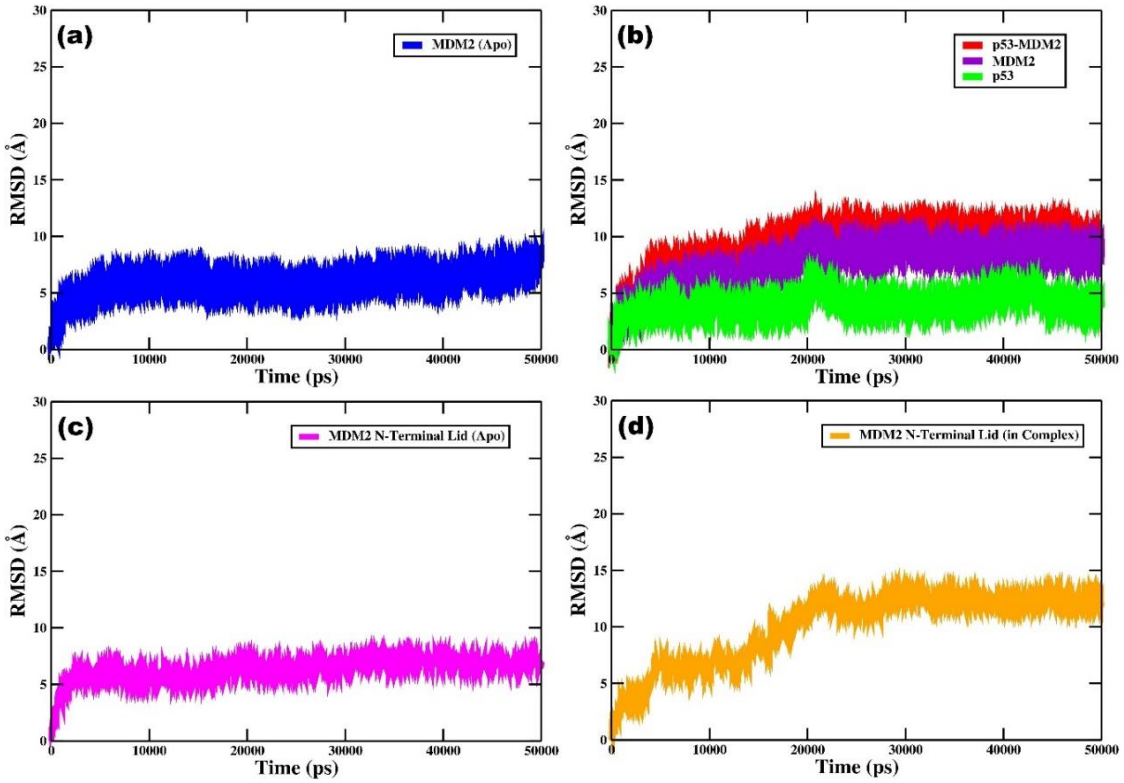

Figure 6.4. *Root Mean Square Deviation analysis for (a) MDM2 (Apo); (b) p53-MDM2 complex; (c) N-Terminal Lid of MDM2 (Apo); and (d) N-Terminal Lid of MDM2 in p53-MDM2 complex.*

6.4.3. RMSF Analysis:

Residue flexibility of the two systems was assessed using the RMSF. **Figure 6.5a** represents the RMSF values for C-α atoms of the MDM2 (Apo) with respect to the time evolution of 50 ns trajectories. **Figure 6.5b** represents the RMSF values for C-α atoms of the individual MDM2 (NTD) and p53 (CTD) with respect to the time evolution of 50 ns

trajectories. For MDM2 (Apo), the residue fluctuations were noticed throughout the C-Terminal residues, and residue fluctuations were observed for N-terminal and C-terminal residues of MDM2 (NTD) and p53 (CTD). Comparing the RMSF of the MDM2 (Apo) with the MDM2 (NTD) present in the p53-MDM2 complex, more number of average residue fluctuations can be observed in MDM2 (NTD) in the complex than in MDM2 (Apo).

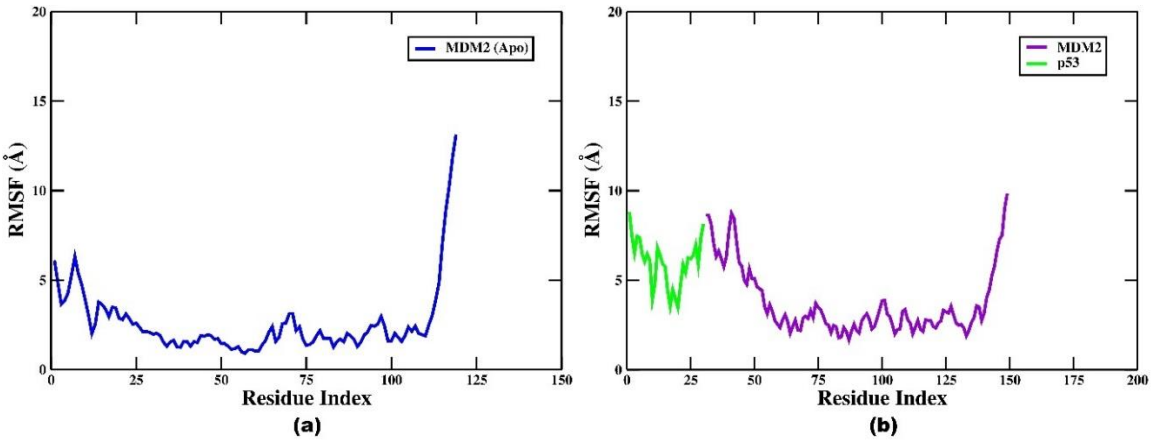

Figure 6.5. *Root Mean Square Fluctuation analysis for (a) MDM2 (Apo); and (b) p53-MDM2 complex.*

6.4.4. Rg Analysis:

Rg is generally calculated to determine the overall dispersion of atoms in a biomolecule from their common center of gravity/axis. The Rg analysis for MDM2 (Apo) and p53-MDM2 complex are shown in **Figure 6.6a** and **6.6b** respectively. Here, it can be observed that the Rg values for MDM2 (Apo) fluctuate within the mean value of 15.5 Å, and the Rg values for p53 (CTD), MDM2 (NTD), and p53-MDM2 complex fluctuate within the mean value of 10 Å, 16 Å, and 19 Å, respectively. The curves for p53 (CTD), MDM2 (NTD), and p53-MDM2 complex were observed to be settled during the entire course of simulation (production dynamics).

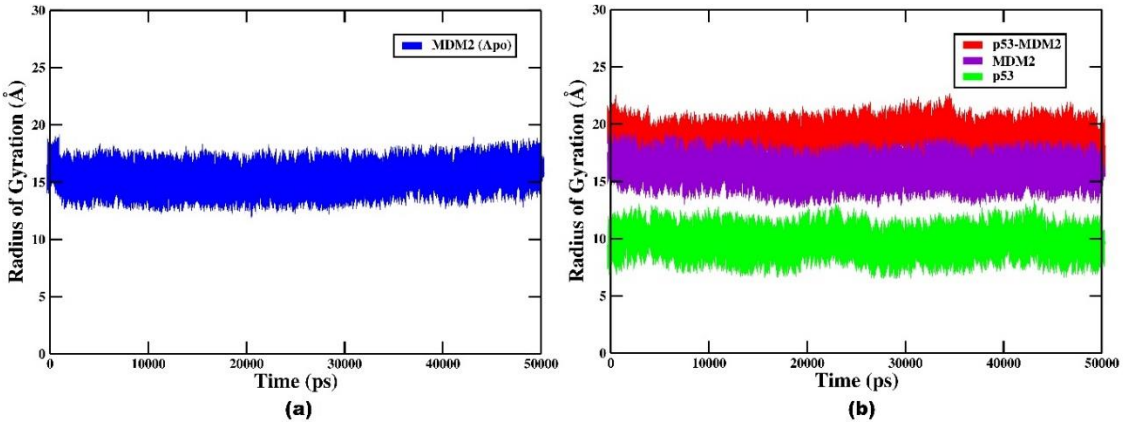

Figure 6.6. *Radius of Gyration analysis for (a) MDM2 (Apo); and (b) p53-MDM2 complex.*

6.4.5. SASA Analysis:

The overall changes in the total SASA of the two systems: MDM2 (Apo) and p53-MDM2 complex are shown in **Figure 6.7a** and **6.7b** respectively. The SASA values are analogous, as well as are directly reflective of the inappropriate (hydrophobic) contacts between the biomolecules and the water molecules. To determine the surface area accessible by the solvent (water) for the two systems, a probe of radius of 1.4 Å was used. The SASA of MDM2 (Apo) was found to be constant at 8500 $Å^2$. The SASAs of the p53 (CTD), MDM2 (NTD) and p53-MDM2 complex were found to be constant at 2000 $Å^2$, 9000 $Å^2$, and 11000 $Å^2$ respectively. Thus, the greater the number of residues, the greater the number of hydrophobic interactions available, and greater will be the SASA value.

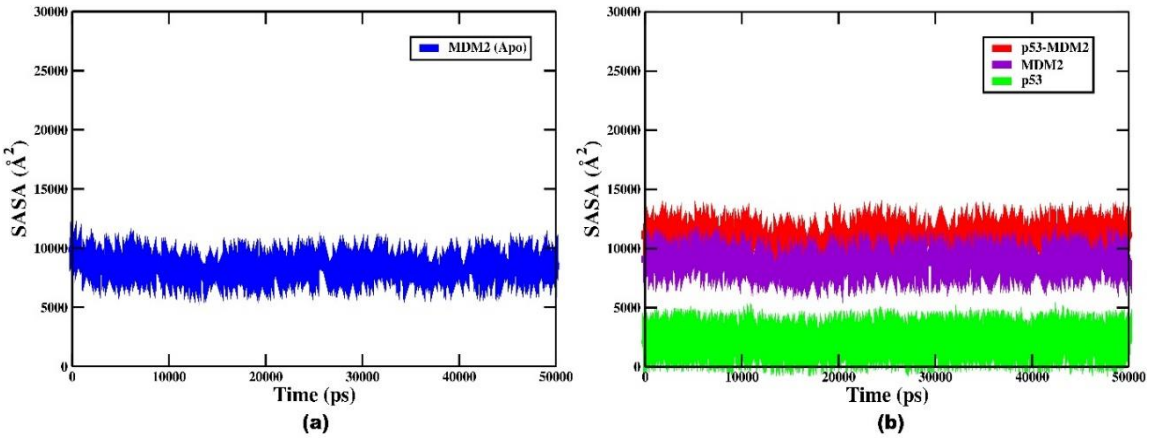

Figure 6.7. *Solvent Accessible Surface Area analysis for (a) MDM2 (Apo); and (b) p53-MDM2 complex.*

6.4.6. Analysis of the Average Distance between the Centers of Mass of the N-Terminal Lid and the N-Terminal Binding Cavity of MDM2:

We also measured the center of mass distance between the N-Terminal binding cavity of MDM2 and the N-Terminal lid of MDM2 for the p53-MDM2 complex. The distance between the N-Terminal binding cavity and the N-Terminal lid was measured as a function of simulation time using their respective trajectory files. From **Figure 6.8**, we can see that the distance between the N-Terminal binding cavity and the N-Terminal lid gradually increases with respect to time.

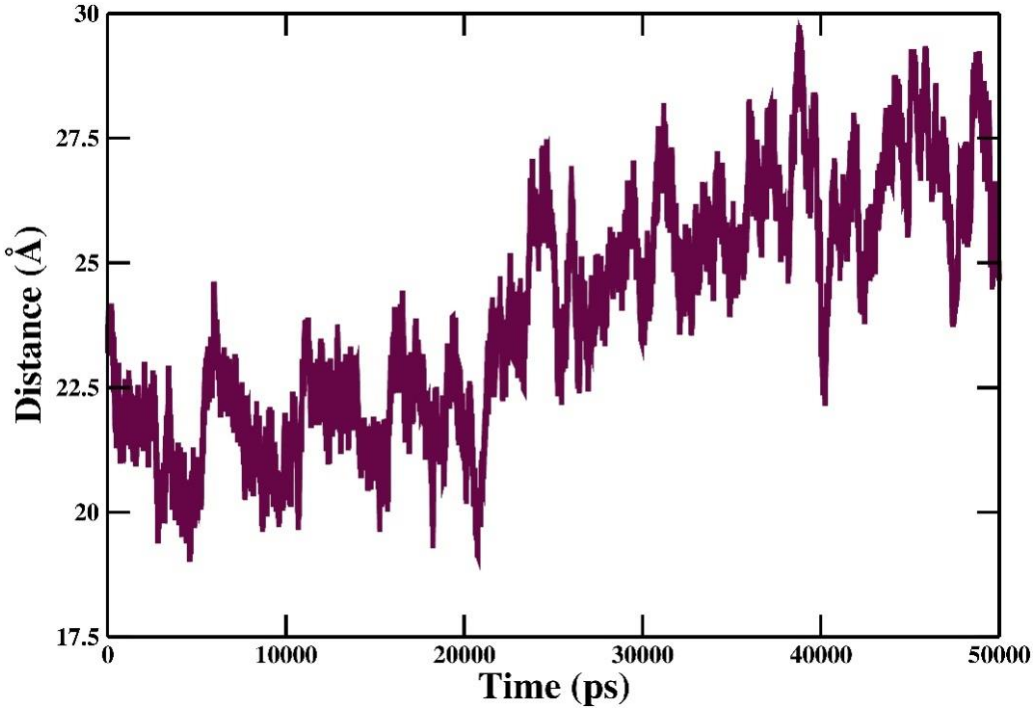

Figure 6.8. *Average distance between the centers of mass of the N-Terminal Lid of MDM2 and the N-Terminal binding cavity of MDM2.*

6.4.7. DSSP Analysis:

Figure 6.9 depicts the secondary structural changes in p53 CTD molecule. From **Figure 6.9**, it can be seen that there is a gradual increase in the α-helix content throughout the course of the simulation. Hence, it can be inferred that the p53 CTD develops a good binding affinity with the MDM2 N-Terminal Lid throughout the simulation.

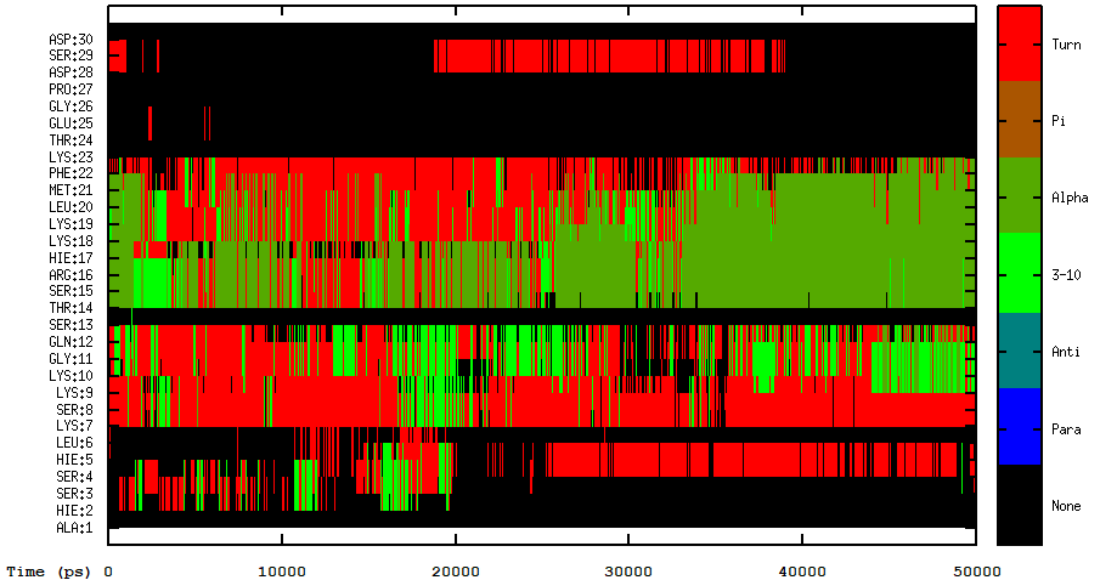

Figure 6.9. *Dictionary of Secondary Structure of Proteins (DSSP) analysis for p53 (CTD). The secondary structure components are color-coded as shown in the panel.*

6.4.8. Secondary structure analysis of the initial and final structures of p53(CTD)-MDM2(NTD) complex:

The secondary structure content of the initial and final structures of the p53 CTD present in the p53CTD)-MDM2(NTD) complex were again determined by uploading the structures in the 2Struc online server. **Table 6.1** represents the secondary structure content of the initial and final structures of p53 CTD.

Table 6.1. *Secondary structure analysis of the initial and final structures of p53(CTD)-MDM2(NTD) complex using 2Struc online server.*

	Helices (%)	***Sheets (%)***	***Turns (%)***
0 ns	*20*	*16.7*	*33.3*
50 ns	*43.3*	*6.7*	*13.3*

6.4.9. Intramolecular Hydrogen Bond Analysis:

The number of intramolecular hydrogen bonds present in p53 (CTD) and in MDM2 (NTD), and the number of intermolecular hydrogen bonds existing in the p53-MDM2 complex were also calculated, as the hydrogen bonds play a significant role in providing the stability to the protein complexes. The hydrogen bonds found were shown in **Figure 6.10a** and **6.10b,** and were observed to have the values within the optimal range

recommended for globular proteins. An average of four inter-molecular hydrogen bonds was found to be present in the p53-MDM2 complex with p53 (CTD) as donor and MDM2 (NTD) as acceptor (**Figure 6.10a**), and an average of five inter-molecular hydrogen bonds was found to be present in the p53-MDM2 complex with MDM2 (NTD) as donor and p53 (CTD) as acceptor (**Figure 6.10b**).

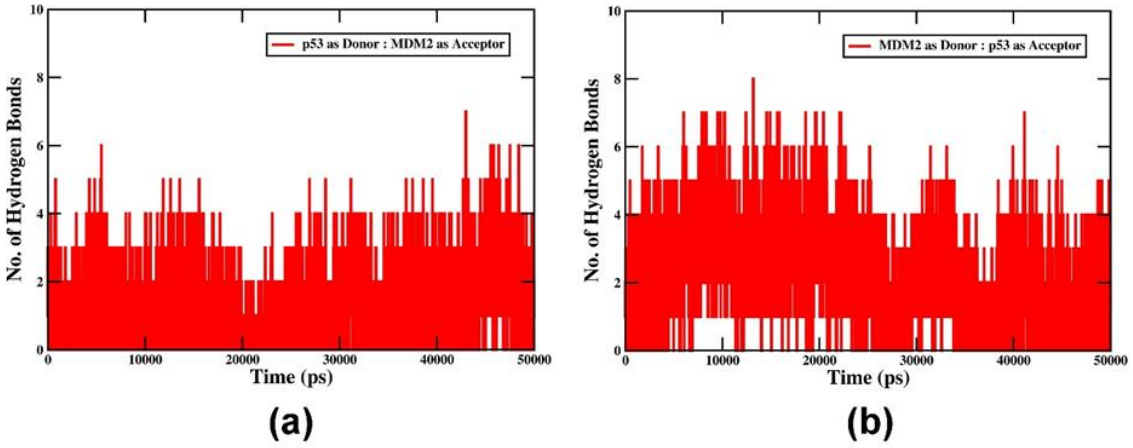

Figure 6.10. *Inter-molecular hydrogen bond analysis of p53-MDM2 complex with (a) p53 as donor and MDM2 as acceptor; and (c) MDM2 as donor and p53 as acceptor.*

6.4.10. Determination of Interface Residues:

An interface area is often described as an area where two sets of proteins get into contact with one another. They are generally characterized by the surface residues with quite large surface areas accessible to the available solvent. The lowest energy structure of the p53(CTD)-MDM2(NTD) complex was retrieved using the RMSD Clustering algorithm from the 50 ns MD trajectories. Then the p53(CTD)-MDM2(NTD) complex was docked with p53 TAD1 using ClusPro 2.0 web server, which was then considered as the system 1. For system 2, the p53(CTD)-MDM2(NTD) complex was superimposed with the p53-MDM2 complex structure downloaded from RCSB PDB (PDB ID: 1YCR), and then the MDM2 NTD (from PDB ID: 1YCR) was removed from the superimposed complex. The p53-MDM2 complex structure downloaded from RCSB PDB (PDB ID: 1YCR) has been considered as the system 3. Three complex systems were submitted to the PDBsum server, to generate the interface statistics. **Table 6.2** represents the interface statistics of p53(TAD1) and MDM2(NTD) in the (a) p53(CTD)-MDM2(NTD) complex docked with p53 TAD1, (b) p53(CTD)-MDM2(NTD) complex superimposed with p53 TAD1 from

the p53-MDM2 complex (PDB ID: 1YCR), and (c) p53-MDM2 complex downloaded from RCSB PDB (PDB ID: 1YCR). The intermolecular interactions between of the three systems have been summarized at the residue levels in **Figure 6.11**.

Table 6.2. Interface statistics of the p53(TAD1)-MDM2(NTD) complex structures.

System	Chain	No. of Interface Residues	Interface Area (Å^2)	No. of Salt Bridges	No. of Disulphide Bonds	No. of Hydrogen Bonds	No. of Non-Bonded Contacts
System 1	MDM2	26	737	-	-	4	580
	p53	13	1142				
System 2	MDM2	26	666	2	-	5	640
	p53	13	1241				
System 3	MDM2	16	660	1	-	3	84
	p53	11	809				

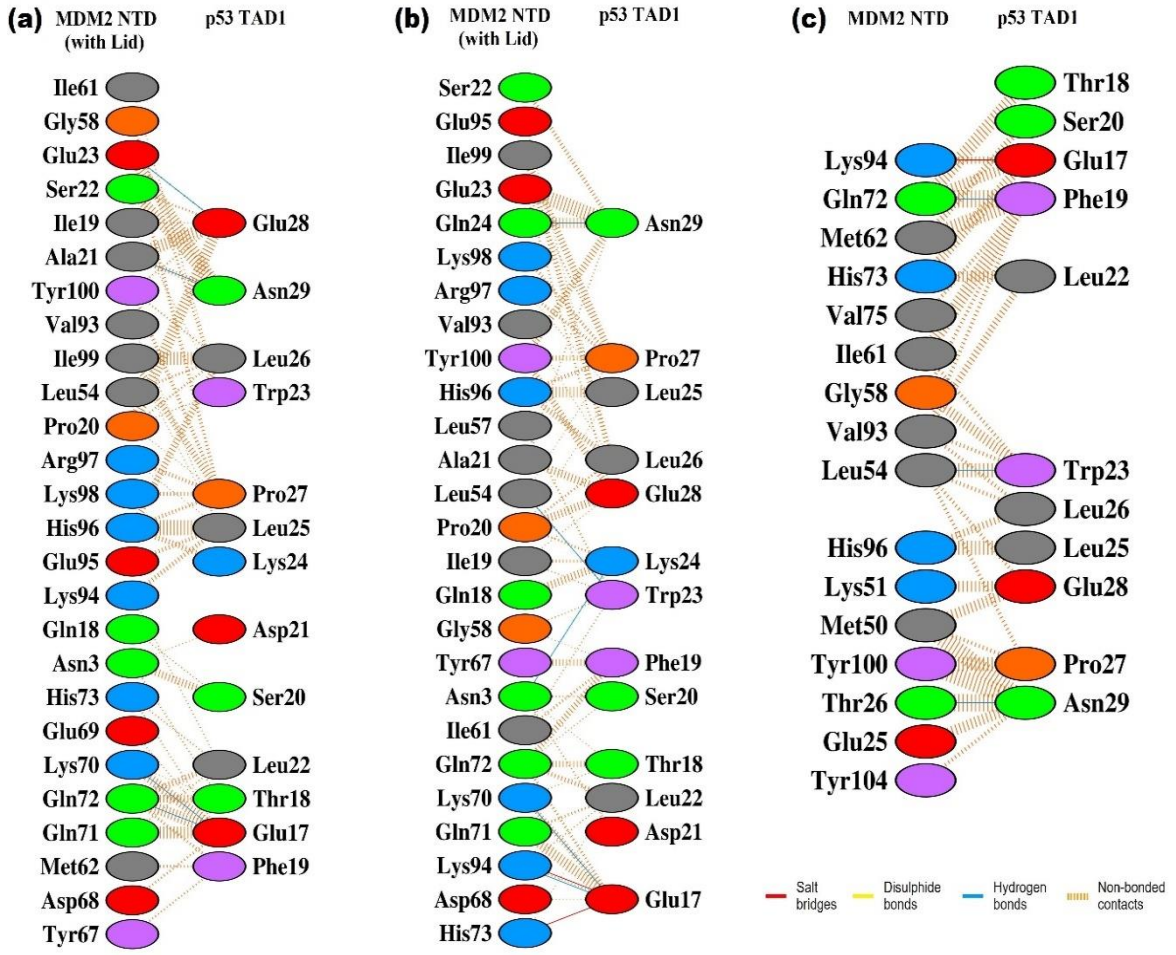

Figure 6.11. *Protein-Peptide Interaction Profile of (a) MDM2 NTD (with Lid) – p53 TAD1 docked complex; (b) MDM2 NTD (with Lid) – p53 TAD1 superimposed complex; and (c) MDM2-p53 complex (PDB ID: 1YCR).*

6.4.11. BFE and PRED Analyses:

The BFE of p53 (CTD) and MDM2 (NTD) to form the p53-MDM2 complex was calculated using the MM/GBSA and MM/PBSA methods. The BFE calculated for the p53-MDM2 complex, along with the various energy terms, are shown in **Table 6.3** and **6.4** respectively.

Table 6.3. *The various components of the BFE (kcal mol^{-1}) evaluated by MM/GBSA method between MDM2 NTD Lid and p53 CTD in the p53-MDM2 complex.*

Components	Complex (kcal mol^{-1})	Standard Deviation (±)	Receptor (kcal mol^{-1})	Standard Deviation (±)	Ligand (kcal mol^{-1})	Standard Deviation (±)	$\Delta\Delta G_{bind}$ (kcal mol^{-1})	Standard Deviation (±)
$\Delta E_{VDWAALS}$	-952.39	13.65	-752.88	11.68	-152.50	3.79	-47.02	3.05
ΔE_{EL}	-10181.81	73.77	-8311.33	54.96	-1810.12	29.49	-60.36	15.97
ΔE_{GB}	-2788.82	62.57	-1723.88	49.72	-1172.01	25.97	107.07	15.46
ΔE_{SURF}	80.48	0.88	66.96	0.78	20.69	0.26	-7.17	0.34
ΔG_{gas}	-11134.20	70.07	-9064.21	51.86	-1962.62	28.56	-107.38	16.64
ΔG_{solv}	-2708.34	62.19	-1656.92	49.33	-1151.33	25.95	99.90	15.24
ΔG_{TOTAL}	-13842.54	27.14	-10721.12	25.91	-3113.94	10.80	**-7.48**	3.29

ΔE_{EL} = electrostatic energy as calculated by the MM force field; $\Delta E_{VDWAALS}$ = van der Waals contribution from MM; ΔE_{GB} = the electrostatic contribution to the polar solvation free energy calculated by GB; ΔE_{SURF} = non-polar contribution to the solvation free energy calculated by an empirical model; ΔG_{gas} = total gas phase energy ($\Delta G_{gas} = \Delta E_{EL} + \Delta E_{VDWAALS}$); ΔG_{solv} = sum of nonpolar and polar contributions to solvation; ΔG_{TOTAL} = final estimated binding free energy in kcal mol^{-1} calculated from the terms above ($\Delta G_{TOTAL} = \Delta G_{gas} + \Delta G_{solv}$).

Table 6.4. *The various components of the Binding Free Energy (kcal mol^{-1}) evaluated by MM/PBSA method between MDM2 NTD Lid and p53 CTD in the p53-MDM2 complex.*

Components	Complex (kcal mol^{-1})	Standard Deviation (±)	Receptor (kcal mol^{-1})	Standard Deviation (±)	Ligand (kcal mol^{-1})	Standard Deviation (±)	$\Delta\Delta G_{bind}$ (kcal mol^{-1})	Standard Deviation (±)
$\Delta E_{VDWAALS}$	-952.39	13.65	-752.88	11.68	-152.50	3.79	-47.02	3.05
ΔE_{EL}	-10181.81	73.77	-8311.33	54.96	-1810.12	29.49	-60.36	15.97
ΔE_{PB}	-2731.77	68.53	-1681.10	54.32	-1116.04	24.82	65.36	14.25
ΔE_{NPOLAR}	1340.92	4.76	1079.35	4.51	300.26	1.51	-38.69	1.74
ΔE_{DISPER}	-941.25	4.30	-762.45	4.25	-249.04	1.51	70.25	2.20
ΔG_{gas}	-11134.20	70.07	-9064.21	51.86	-1962.62	28.56	-107.38	16.64

ΔG_{solv}	-2332.09	69.61	-1364.18	54.94	-1064.82	25.05	96.91	14.79
ΔG_{TOTAL}	-13466.29	28.01	-10428.39	27.82	-3027.44	11.02	**-10.46**	6.58

ΔE_{EL} = electrostatic energy as calculated by the MM force field; $\Delta E_{VDWAALS}$ = van der Waals contribution from MM; ΔE_{PB} = the electrostatic contribution to the polar solvation free energy calculated by PB; $\Delta E_{NPOLAR}+\Delta E_{DISPER}$ = non-polar contribution to the solvation free energy calculated by an empirical model; ΔG_{gas} = total gas phase energy ($\Delta G_{gas} = \Delta E_{EL}+\Delta E_{VDWAALS}$); ΔG_{solv} = sum of nonpolar and polar contributions to solvation; ΔG_{TOTAL} = final estimated binding free energy in kcal mol^{-1} calculated from the terms above ($\Delta G_{TOTAL} = \Delta G_{gas}+\Delta G_{solv}$).

From **Table 6.3** and **6.4**, it can be observed that all the derived components for the BFE analysis contributed to the binding of p53 (CTD) and MDM2 (NTD) to form the p53-MDM2 complex. The $\Delta G_{binding}$ for the p53-MDM2 complex calculated using MM/GBSA gives a value of -7.48 kcal mol^{-1}, and the $\Delta G_{binding}$ for the p53-MDM2 complex calculated using MM/PBSA gives a value of -10.46 kcal mol^{-1}.

For the better understanding of the protein-protein binding process, the contribution of each individual residue to the BFE has been studied in depth. To create the residue-residue interaction spectrum, the BFE has been decomposed in terms of interacting residue-residue pairs. The residue decomposition process is particularly effective for describing the protein-protein binding mechanism at the atomic level, as well as analysing the contribution of each individual residue to the BFE. The contribution of numerous key residue-residue pairs toward BFE have been shown in **Figure 6.12**. **Figure 6.12a** and **6.12b** represent the PRED analysis for p53 and MDM2 respectively, calculated using MM/GBSA method. **Figure 6.12c** and **6.12d** the PRED analysis for p53 and MDM2 respectively, calculated using MM/PBSA method. From **Figure 6.12a** and **6.12b**, it can be observed that residues MET21, HIE17, andLYS23 from p53 (CTD), and residues ASN5, VAL14, and PRO9 from MDM2(NTD) make a substantial contribution towards the BFE calculated using MM/GBSA. From **Figure 6.12c** and **6.12d**, LYS10, MET21, and LYS23 from p53 (CTD), and MET1, ASN5, and SER7 from MDM2 (NTD) are observed to make a substantial contribution towards the BFE calculated using MM-PBSA.

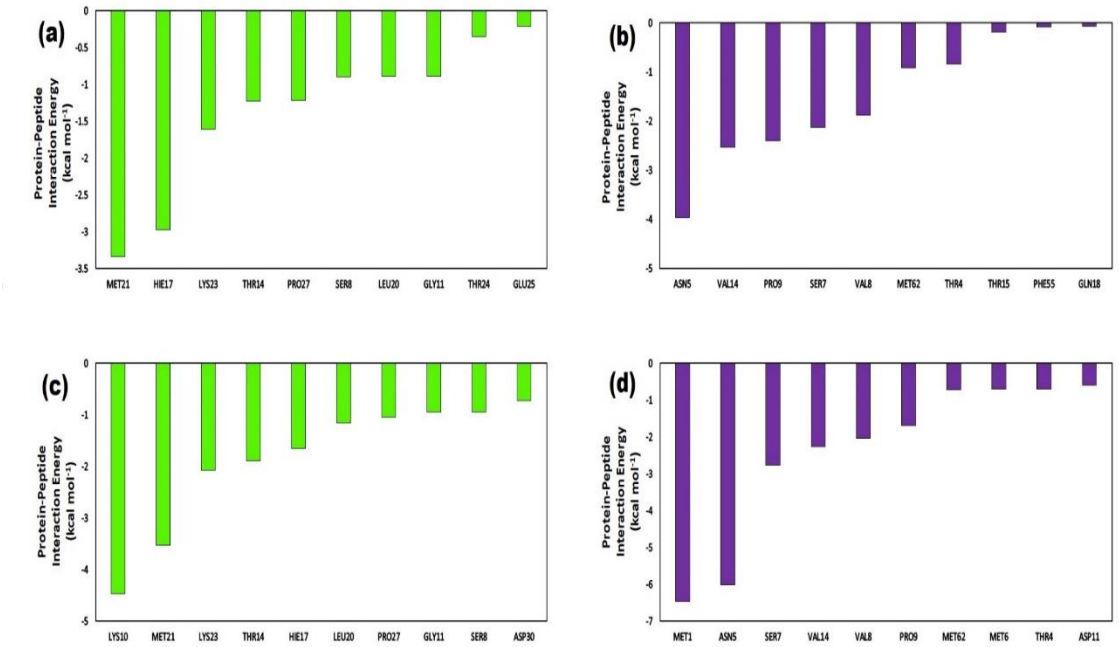

Figure 6.12. *Per Residue Energy Decomposition analysis for (a) p53 and (b) MDM2 calculated using MM/GBSA method, and for (c) p53 and (d) MDM2 calculated using MM/PBSA method.*

6.5. Conclusion:

In this work, we have studied the conformational dynamics and stability of the NTD of MDM2 with the lid, and the p53(CTD)-MDM2(NTD) complex have been studied using MD simulation. The production dynamics was carried out for 50 ns. the NTD of MDM2 with the lid (in apo state) was found to be in closed conformation throughout the simulation. On the other hand, the N-Terminal lid in the p53(CTD)-MDM2(NTD) complex was found to get displaced during the simulation, resulting in the transformation of the the initial closed conformation of the p53(CTD)-MDM2(NTD) complex to an open conformation at the end of the simulation. Then the p53 TAD1 structure obtained from the pdb structure downloaded from RCSB PDB (PDB ID: 1YCR) was docked with the lowest energy structure of the p53(CTD)-MDM2(NTD) complex. The lowest energy structure of the p53(CTD)-MDM2(NTD) complex was found to be present an open conformation. The p53 TAD1 was found to fit perfectly into the N-Terminal binding cavity of MDM2. We then measured the average distance between the CoMs of the N-Terminal Lid and the N-Terminal Binding cavity of MDM2 throughout the simulation for the p53(CTD)-MDM2(NTD) complex, which was found to increase during the simulation. From the DSSP analysis of p53(CTD) present in the p53(CTD)-MDM2(NTD)

complex, it was found that there is a gradual increase in the α-helix content during the simulation, resulting in a good binding affinity between p53(CTD) and MDM2(NTD). We also carried out the BFE as well as PRED analyses for the complex. A good binding affinity between p53 (CTD) and MDM2 (NTD) was found (-7.48 kcal mol^{-1} calculated using MM/GBSA, and -10.46 kcal mol^{-1} calculated using MM/PBSA). The highlights from our work may be useful in designing novel potential inhibitors of p53-MDM2 interactions.